Check for updates

A drought monitoring framework for data-scarce regions

Roberto A. Real-Rangel, Adrián Pedrozo-Acuña, J. Agustín Breña-Naranjo and Víctor H. Alcocer-Yamanaka

ABSTRACT

Drought monitoring is a critical activity for drought risk management; however, the lack of ground-based observations of climatological and hydrological variables in many regions of the world hinders an adequate follow-up and investigation of this phenomenon. This paper introduces a transparent framework for monitoring the spatio-temporal distribution of drought hazard based on uni- and multivariate standardized drought indices that use reanalysis datasets of hydrological variables available freely and globally. In the case study of the 2015–2017 East-Southwest drought in Mexico, the introduced framework successfully detected the spatial and temporal patterns of drought conditions, even in regions where a benchmark drought monitoring system failed to detect deficits. In addition, the ability of the introduced framework to detect drought impacts on the annual agricultural maize production in Mexico was evaluated using data of 1980–2018, yielding scores of the false alarm ratio =0.32, the probability of detection = 0.71, and the proportion correct = 0.68 for the analysis at the national scale. Currently, the framework provides a significant extension to the capabilities for national drought monitoring, and it is being used by the Mexican water authority in the decision-making process related to drought severity assessment.

Key words | drought monitoring, Mexico, Multivariate Standardized Drought Index (MSDI), Standardized Precipitation Index (SPI), Standardized Runoff Index (SRI), Standardized Soil Moisture Index (SSI)

Roberto A. Real-Rangel (corresponding author)
Adrián Pedrozo-Acuña
J. Agustín Breña-Naranjo
Institute of Engineering,
National Autonomous University of Mexico,
Circuito Escolar s/n, Ciudad Universitaria,
Coyoacan, CDMX, Mexico 04510,
Mexico
E-mail: *rrealr@iingen.unam.mx*

Roberto A. Real-Rangel
Program of Master and Doctorate in Engineering,
National Autonomous University of Mexico,
Universidad 3000, Ciudad Universitaria, Coyoacan,
CDMX, Mexico 04510,
Mexico

Víctor H. Alcocer-Yamanaka
National Water Commission,
Insurgentes Sur 2416, Copilco El Bajo, Coyoacan,
CDMX, Mexico 04340,
Mexico

INTRODUCTION

Droughts are a temporary, recurrent event originating from the lack of precipitation that has potential effects on the water availability in a hydrologic system (Smakhtin & Schipper 2008). Although they are a typical feature of any climate, they might have negative consequences on a wide range of social, economic, and environmental sectors (Stahl *et al.* 2016). The severity of these impacts is directly related to the severity of the drought, but it is the lack of an adequate drought risk management that might turn an event into a disaster (Blauhut *et al.* 2016). Thus, efforts dedicated to reducing drought risk are generally oriented to protect and minimize the vulnerability of the human and environmental systems, including actions like monitoring natural indicators.

Drought monitoring consists of the compilation and analysis of data from natural variables associated with the onset, persistence, and termination of droughts (e.g., precipitation, runoff, and soil moisture) to quantify drought indices and communicate them to decision makers and the public (Wilhite 2000). Through drought indices, it is possible to characterize the severity of events, for which one of the most widely used approaches is the method of the reference level (Yevjevich 1967) based on the theory of statistical runs. This approach consists in selecting a reference value of a

doi: 10.2166/hydro.2019.020

Downloaded from http://iwaponline.com/jh/article-pdf/22/1/170/642272/jh0220170.pdf
by guest

given drought indicator or an index from which deviations will be analyzed: the greater the negative deviation, the more intense the deficit of water. A negative run, interpreted as a period of deficit, starts when the variable analyzed crosses the reference value downwards, and it lasts until a new value above the reference occurs. The time between the start and end of the run is the drought *duration*; the sum of the deviations during the deficit period is known as the *magnitude* of the drought, and the ratio of the magnitude to the duration is the *mean intensity* of the event (Figure 1). Duration, magnitude, and intensity are the basic temporal characteristics for drought definition.

While there is no such thing as 'the best drought index', for sake of operability, drought monitoring requires performing a selection of the more than 100 indices available in the literature, ideally based on criteria such as robustness, tractability, and transparency (Keyantash & Dracup 2002). Besides, this selection should also consider the drought aspect intended to be detected, such as the meteorological origins of the drought (meteorological drought), the agricultural impacts of droughts (agricultural drought), or the effects of dry spells on surface, subsurface, and groundwater hydrology (hydrological drought) (Wilhite & Glantz 1985). The signature of drought may be lagged during its passage through the catchment, provoking delays between the onsets of the different types of droughts, prolonging the duration, and attenuating the intensity of the anomalies in a process known as drought propagation (van Loon 2013). Following this rationale, a single drought indicator may not be sufficient to characterize the complex drought conditions (Hao & Singh 2015), which has motivated the use of indicators of different stages of the hydrological cycle in many drought monitoring systems.

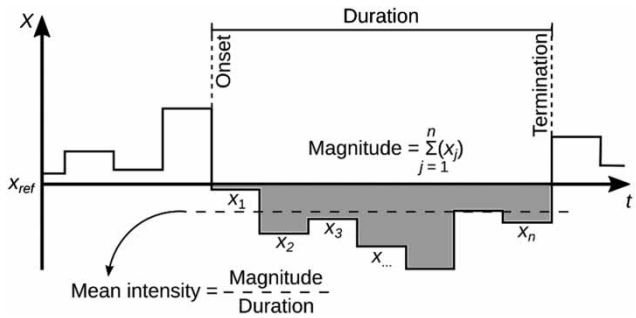

Figure 1 | Definition of the basic features of droughts.

There are several drought monitors at global, continental, and regional scales, differing in their data sources, spatial and temporal resolution, and the drought indices applied. For example, the Global Integrated Drought Monitoring and Prediction System (GIDMaPS; Hao *et al.* 2014; http://drought.eng.uci.edu), supported by the University of California Irvine, derived data of precipitation and soil moisture from NASA's reanalysis product MERRA-Land to compute three drought indices on a global scale: the Standardized Precipitation Index (SPI; McKee *et al.* 1993), the Standardized Soil Moisture Index (SSI; Hao & AghaKouchak 2013), and the Multivariate Standardized Drought Index (MSDI; Hao & AghaKouchak 2013). Authors demonstrated that the system successfully detected severe droughts like the Amazon, the Russian, and the Texas-Mexico droughts in 2010 and the East Africa drought of 2011; unfortunately, the production of GIDMaPS was interrupted on February 2016 when the MERRA-Land product was also discontinued. The European Drought Observatory (EDO; Sepulcre-Canto *et al.* 2012; http://edo.jrc.ec.europa.eu) of the European Commission reports a Combined Drought Indicator (CDI) that evaluates the degree of drought hazard for agriculture in Europe based on the SPI, anomalies in an indicator of soil moisture derived from a hydrological model, and the anomalies in a remote sensing-derived indicator of biomass and vegetation condition. These variables and indices are combined with different time-lags and aggregation periods to capture the temporal development of droughts, firstly detected in early precipitation deficits, then in the soil moisture and, finally, in their impacts on the vegetation conditions, to assess the severity level. Its capabilities for detecting events on a regional scale were qualitatively tested with the European drought of 2011, identifying the different stages of the agricultural drought in the most affected areas. The United States Drought Monitor (USDM; Svoboda *et al.* 2002; https://droughtmonitor.unl.edu/) reports a series of maps of drought indices and indicators, including the Palmer Drought Severity Index (PDSI; Palmer 1965), percentiles of soil moisture and daily streamflow, the percent of normal precipitation, and the SPI, among others. Likewise, it presents a map of the result of a process that involves the objectively weighted average of drought indices and the input of regional and local experts to define the affected regions.

Downloaded from http://iwaponline.com/jh/article-pdf/22/1/170/642272/jh0220170.pdf
by guest

In Mexico, since 2003, the National Meteorological Service of the National Water Commission (SMN-CONAGUA) has replicated the methodology of the USDM for Mexico: first, as a part of the North American Drought Monitor (NADM; Lawrimore *et al.* 2002; https://www.ncdc.noaa.gov/temp-and-precip/drought/nadm/) and, from 2014 on, also in the independent system Drought Monitor in Mexico (MSM; Lobato-Sánchez 2016; https://smn.conagua.gob.mx/es/climatologia/monitor-de-sequia/monitor-de-sequia-en-mexico). However, the procedure by which the USDM methodology is applied in Mexico differs from the original in two main aspects: the available input data for computing the drought indices and the indices blending procedure. The MSM derives precipitation and temperature data from the CONAGUA's Climatological Database, using only sites with at least 30 years of records and with less than 20% of missing data. The spatial density of the resultant subset (with 415 stations currently) does not meet the minimum recommendations for managing water resources (WMO 2009). Figure 2(a) shows a Voronoi diagram where each polygon encloses the region for which each station is the nearest available. It can be derived that 86% of the stations cover a region that exceeds 900 km^2, recommended for the least dense classification (coastal regions), excluding the polar/arid zone. This is a drawback for the robust methodology of the USDM, which may become weaker if only a few inputs are available (WMO & GWP 2016).

On the other hand, the MSM also incorporates the percent of storage available in the principal reservoirs of the country as a drought indicator. Figure 2(b) includes the basins of the 172 reservoirs monitored, which cover 36% (693,606 km^2) of the Mexican territory. Nevertheless, 62 of the reservoirs with the largest basins receive discharges influenced by the presence of hydropower- or irrigation-dams upstream, which might provoke a misrepresentation of the hydro-climatological conditions of the region. The main effect of these controls on drought characteristics is the attenuation of the intensity, and the lagging and prolongation of the drought period when propagating a deficit in precipitation in the basin to a deficit in streamflow (Wu *et al.* 2016), hindering the efficiency of the available storage in reservoirs as a drought indicator.

Besides the limitations of the inputs used, the methodology applied in the MSM is not transparent in that the weights used in the average of drought indicators are assigned subjectively by the climatology expert performing the analysis (Lobato-Sánchez 2016). This subjectivity inherited from the USDM methodology might be seen as an issue when using drought maps resulting from this procedure as the basis for decision-making for assigning resources to aid drought-affected regions (Kao & Govindaraju 2010). This is the case for Mexico, where CONAGUA, the highest authority in the water resources management, issues official opinions on drought conditions, based on the results of MSM, which are used by the Interior Ministry (SEGOB) to allocate financial resources (SHCP 2010).

This paper introduces a transparent framework for generating drought monitoring products in Mexico that applies a simple, reproducible methodology that derives

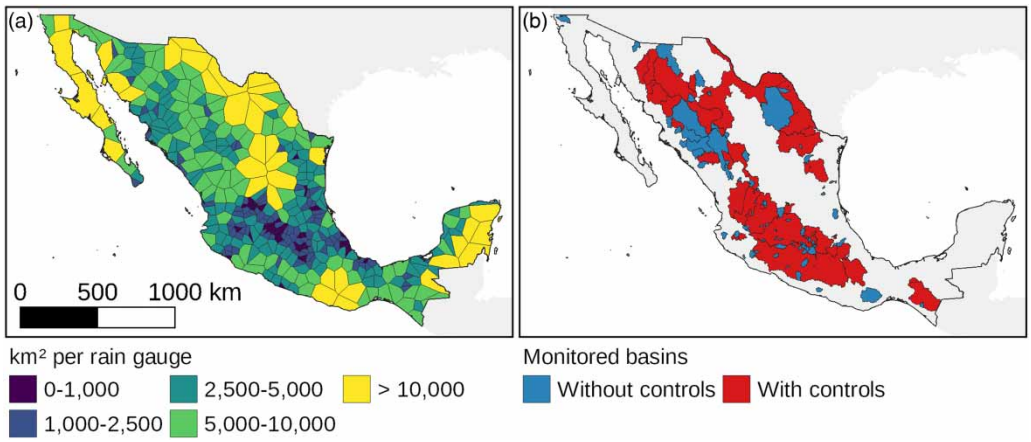

Figure 2 | Networks of direct observations used for drought monitoring in the MSM: (a) density of climatological stations and (b) basins of monitored reservoirs.

Downloaded from http://iwaponline.com/jh/article-pdf/22/1/170/642272/jh0220170.pdf
by guest

hydrological variables from a freely and globally available reanalysis product to compute a set of Standardized Drought Indices (SDI) at a regional scale based on the principle of the SPI.

DATA

The drought monitoring framework introduced in this paper uses as input monthly hydrological data from NASA's reanalysis product Modern-Era Retrospective Analysis for Research and Applications, version 2 (MERRA-2; Gelaro *et al.* 2017). MERRA-2 simulates the atmosphere dynamics with an atmospheric general circulation model (AGCM) and reproduces the exchange of water and energy fluxes between the atmosphere and the land surface with the land surface model (LSM) Catchment (Koster *et al.* 2000). Its datasets are available from January 1980 to the present, with a spatial resolution of $5/8^\circ \times 1/2^\circ$, and are published with a latency of 18–20 days in the website of the Goddard Earth Sciences Data and Information Services Center (GES DISC; https://disc.gsfc.nasa.gov). Although this latency period hinders using the product for real-time monitoring, given the slow-onset and creeping nature of this phenomenon, it is well suited for representing ongoing drought conditions.

The AGCM forces the LSM with precipitation, radiation, and near-surface air temperature and humidity, among other variables. In turn, the LSM delivers fluxes of moisture and energy to the AGCM, updating in the process its internal moisture and energy states (Reichle *et al.* 2017a). In the framework presented here, drought is monitored through the anomalies in precipitation (PRECTOTLAND), soil moisture in the root zone (RZMC), and the sum of overland flow, throughflow, and baseflow (RUNOFF + BASEFLOW), stored in the Land Surface Diagnostics MERRA-2 data collection (M2T1NXLND).

PRECTOTLAND is the precipitation flux generated with the AGCM and corrected with gauge- and satellite-based precipitation observations. The variability of RZMC is estimated by the LSM based on the transfers of moisture between three levels of the soil: the surface soil, the root zone, and the vadose zone. These transfers work to keep the system close to the assumed equilibrium soil moisture profile in the unsaturated zone. Evaporation and runoff processes are represented with different models depending on the distribution of the RZMC; for example, if a storm occurs in a saturated region, all the throughfall is converted to overland flow (RUNOFF); on the other hand, in a region where RZMC is subsaturated, but above the vegetation-specific wilting point, the precipitation contributes to RUNOFF only if there is an excess in its surface soil moisture. Finally, BASEFLOW is directly controlled by the mean water table depth in the catchment, defined through the moist transfers described above, and the mean of the topographic index in the catchment, computed at each point as $\ln(a/\tan\beta)$, with a being the upstream area that contributes flow to the given point and β being the local slope angle.

The performance of land surface variables of MERRA-2 was recently tested by Reichle *et al.* (2017b) against *in situ* measurements. In a comparison of the seasonal mean PRECTOTLAND against the Global Precipitation Climatology Project product, version 2.2 (GPCPv2.2; Adler *et al.* 2003; https://precip.gsfc.nasa.gov/gpcp_v2.2_data.html), it was found that the average magnitude of the bias for the period December–February is 0.7 mm day^{-1} and for June–August, 1.1 mm day^{-1}. Besides, an evaluation of the correlation coefficients (R) between monthly time series of both products in the period of 1979–2015, a global average R of 0.82 was found. Meanwhile, the root zone moisture field exhibits an unbiased root-mean-square error of 0.04 m^3 m^{-3} and an average R of 0.71 when compared to ground-based measurements in the USA, France, and Australia. Finally, reanalysis runoff estimates, compared to naturalized monthly streamflow gauge data in the USA, present skill values (anomaly R) ranging from 0.5 to 0.9.

METHODS

The framework presented here is synthesized as shown in Figure 3. The following subsections describe the components of the analysis pipeline.

Drought definition

Monitoring products generated with this framework use the SDI approach to quantify drought features based on the

Downloaded from http://iwaponline.com/jh/article-pdf/22/1/170/642272/jh0220170.pdf
by guest

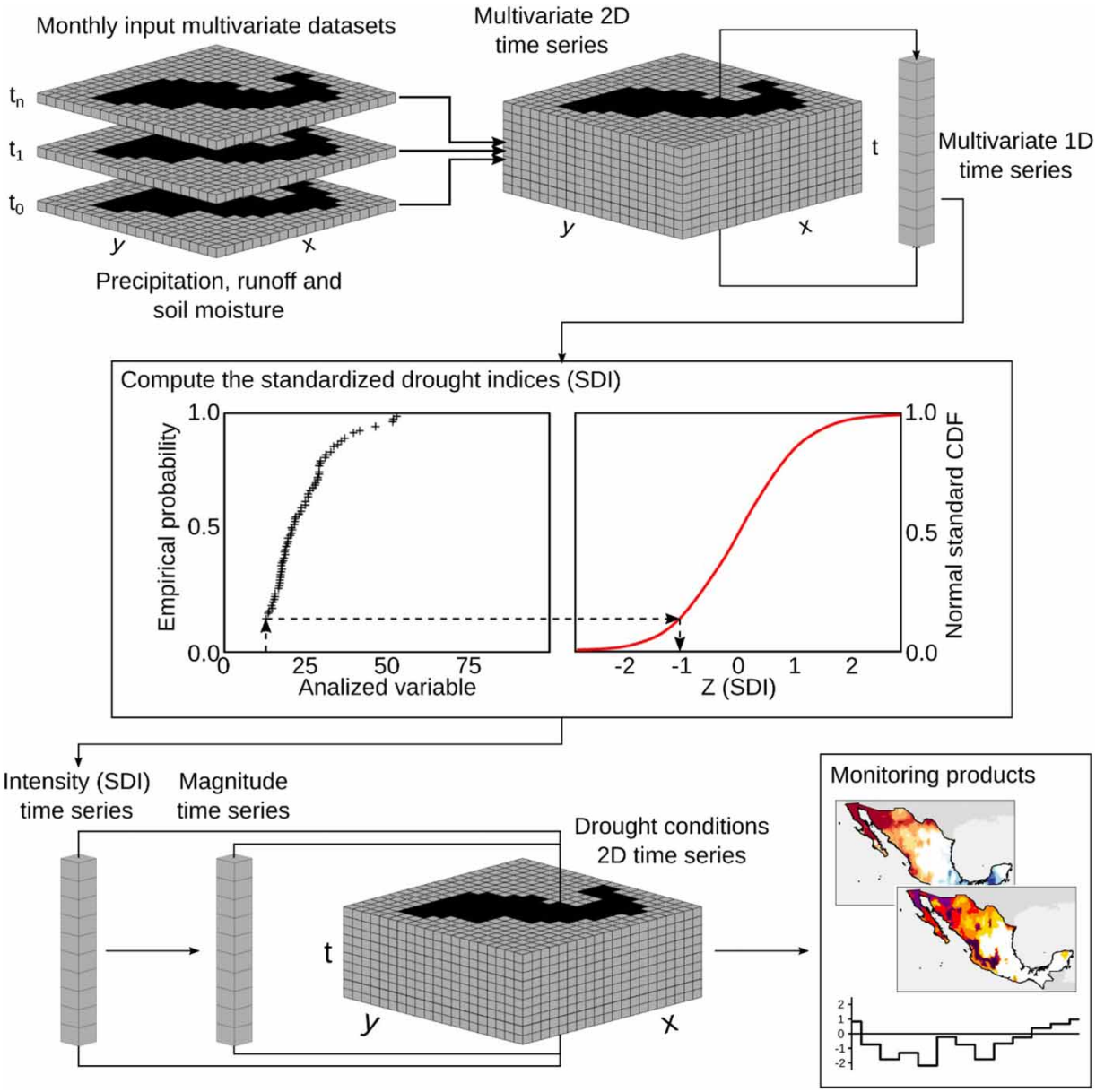

Figure 3 | Analysis pipeline of the monitoring framework proposed.

procedure originally proposed for the SPI. To calculate the SPI, a long-term precipitation record is fitted to a probability distribution, which is then normalized applying the inverse normal standard distribution. The resulting Z value for each observed precipitation is the SPI. Negative (positive) values of SPI are interpreted as a negative (positive) deviation from regular conditions; the higher the absolute value, the greater the intensity of the deviation. After its publication in 1993, the SPI methodology has been applied to other variables. For example, Hao & AghaKouchak (2013) found that the SSI captures the lagged onset of the deficit of soil moisture and the prolongation of the dry periods compared with the SPI. Likewise, Shukla & Wood (2008) observed similar results with the Standardized Runoff Index (SRI) that presented less variability than the SPI, resulting in longer periods of deficit of runoff than those of deficit of precipitation.

While powerful, the SPI has the drawback of being highly sensitive to the choice of the probability distribution

Downloaded from http://iwaponline.com/jh/article-pdf/22/1/170/642272/jh0220170.pdf
by guest

function. Quiring (2009) found significant differences between SPI values calculated using the Pearson type III and the two-parameter gamma PDFs, mainly in the extreme values ($|\text{SPI}| \geq 1.5$), where mean absolute deviations ranging from 0.18 to 0.29 were found. This inconsistency hinders the comparison of drought conditions between regions where SPI uses different PDFs. In this regard, Farahmand & AghaKouchak (2015) proposed a workaround for this issue by using the empirical probability of each value in the long-term record, which is then transformed to the normal standard distribution, resulting in a nonparametric SDI. To this end, they used the following plotting position formula:

$$p(x_k) = \frac{m - 0.44}{n + 0.12} \tag{1}$$

and then

$$\text{SDI} = \phi^{-1}(p) \tag{2}$$

where x_k is a given value in the long-term record of the variable X; n is the size of the sample; m is the number of occurrences of the value x_i for $x_i \leq x_k$; and ϕ is the standard normal distribution function.

The use of univariate drought indices along with multivariate indices offers a framework useful for risk assessment and management for a wide range of sectors, such as agriculture, hydropower generation, and public water supply, while keeping attention on the process of propagation of the deficit throughout the catchment. In this sense, Hao & AghaKouchak (2013, 2014) proposed the MSDI as an extension of the SDI approach to assess multiple variables using a single index, allowing the study of drought features from a broader view to detect different phases of a drought event, such as its onset and persistence. The non-parametric approach already described can also be applied in the MSDI, using the multivariate form of Equation (1), to compute $p(x_k, y_k, \ldots)$, where x and y would be two variables related to a phase of a drought; n is the number of sets $(x, y, \ldots)$ in the sample; and m is the number of occurrences of the set $(x_i, y_i, \ldots)$ for $x_i \leq x_k$ and $y_i \leq y_k$. An implicit effect of this methodology is to present more intense deficits when more than one of the considered variables detect, marginally, deficit conditions. This characteristic may be understood as the result of the effect of two (or more) threads acting simultaneously over an exposed system, which might be the desired behavior. However, it must be kept in mind when interpreting the results of MSDIs that negative values of this index are more probable (Erhardt & Czado 2018). This might be corrected by using lower intensity thresholds for the MSDIs than the other SDIs; however, that measure has not been explored in this analysis.

The monitoring framework presented here computes three univariate and three multivariate SDIs using the described approach: the SPI, for precipitation; the SRI, for runoff; the SSI, for soil moisture; the MSDI, for the combination of precipitation and runoff (MSDI_{PR}), precipitation and soil moisture (MSDI_{PS}), and precipitation, soil moisture, and runoff (MSDI_{PRS}). The different MSDIs allow us to detect and characterize drought events simultaneously through multiple phases of the hydrological cycle in the land surface, while the SPI, SSI, and SRI quantify deficits in each of its components. Furthermore, the SDIs are computed for different periods of temporal aggregation to provide drought monitoring products for analyses and decision-making support in different temporal scales.

The reference level that separates excess and deficit values in SDIs is 0.0; however, deviations from this reference lack a physical interpretation. Hence, to allow a clearer communication of the drought conditions, negative values of SDIs are usually classified as shown in Table 1.

This framework also computes the monthly drought magnitude, which represents the accumulated deficit since the onset of an event. McKee *et al.* (1993) reported the value of this indicator divided over an intensity threshold and interpreted its result as the drought duration if each

Table 1 | Drought intensity classification (modified from Svoboda *et al.* 2002)

Category	SDI range	Percentile chance
Exceptional drought (D4)	$\text{SDI} \leq -2.0$	$P \leq 2$
Extreme drought (D3)	$-2.0 < \text{SDI} \leq -1.6$	$2 < P \leq 5$
Severe drought (D2)	$-1.6 < \text{SDI} \leq -1.3$	$5 < P \leq 10$
Moderate drought (D1)	$-1.3 < \text{SDI} \leq -0.8$	$10 < P \leq 20$
Abnormally dry (D0)	$-0.8 < \text{SDI} \leq -0.5$	$20 < P \leq 30$

Downloaded from http://iwaponline.com/jh/article-pdf/22/1/170/642272/jh0220170.pdf
by guest

month of the drought has the value of that threshold. Here, a threshold of 1.3 is adopted, which is the absolute value of intensity categorized as a 'severe drought' (see Table 1). Also, an arbitrary classification of its values is proposed to make maps of drought magnitude (M) clearer: M1 ($1 \leq M < 3$), M2 ($3 \leq M < 6$), M3 ($6 \leq M < 9$), M4 ($9 \leq M < 12$), and M5 ($M \geq 12$). Most of the regional and global drought monitoring systems do not include the drought magnitude as a monitoring product (see, for example, the GIDMaPS). This product would give insight into the progressive aggravation of drought conditions until the present, which might be helpful to define the priority of attention, especially for long-term impacts, like hydrological or ecological, even in the case when present intensity is not particularly high.

Data processing

Literature reports informatic tools to compute SDIs. For example, Farahmand & AghaKouchak (2015) introduced the open source package Standardized Drought Analysis Toolbox (SDAT) for MATLAB (available at http://amir.eng.uci.edu/sdat.php), which applies the nonparametric approach to compute uni- and multivariate SDIs on which the present framework is based. Their software allows only time series as inputs which leaves the alternative of implement SDAT in a loop structure throughout the region of interest; however, this approach becomes inefficient when working in regions formed by many grid cells. Besides, although the code is openly available, it is written in a proprietary programming language for the commercial software MATLAB, which requires purchasing a license. Tigkas *et al.* (2014) presented the Drought Indices Calculator (DrinC), programmed in Visual Basic 6. In contrast to the SDAT, DrinC has a full graphical user interface, which makes it more user-friendly. This tool computes the SPI, among other drought indices, based on time series data including the option of entering data from multiple points to compute the drought indices in a loop structure, using an approach similar to that of SDAT. However, given that the source code is not available, DrinC cannot be implemented as a part of a programming script, which would expedite setting the input data in the format required by the software.

Land Surface Diagnostics data collection of MERRA-2 contains 50 variables of flux and state of water and energy, for the almost 208,000 grid cells of the globe, stored in 1-month files in the Network Common Data Form (NetCDF) format of 196 MB each, summing more than 92 GB of data in all its temporal coverage (January 1980 to present). This amount of data might represent a limitation for its processing in a commercially available personal computer with constrained specifications due to the memory needed to load the data and perform calculations with it.

In this scenario, it was necessary to develop a set of scripts to process the input datasets and compute the SDIs optimizing the use of the computer resources. This framework processes MERRA-2 multivariate data taking advantage of recent developments of Python packages for geosciences, using the *xarray* package (Hoyer & Hamman 2017), which, in turn, uses the out-of-core analysis of datasets of the *Dask* library (Rocklin 2015). The *xarray* library implements data structures and an analytics toolkit for multidimensional labeled arrays based on the data model on which the NetCDF format is built. This package allows, among other key features, resampling and aggregating data along a specific dimension, which is used to compute the SDI for different temporal scales. On the other hand, the *Dask* package allows us to use the disk as an extension of the memory, which makes it possible to perform calculations with arrays of data bigger than the memory of the computer.

The software developed performs the following steps. First, the monthly datasets of MERRA-2 are combined into a single multivariate 2D time series. Then, the uni- and multivariate SDIs are computed in each cell in the analyzed area, using as input its associated time series. After this, the drought magnitude is derived by accumulating the values of the SDIs of each time step until a shift in the sign of the values of intensity is detected. Finally, the data arrays of intensity and magnitude are merged into one multivariate 2D time series, which is then exported as a spatial dataset in the NetCDF format that can be easily visualized or used to compose maps in the most widely used geographic information systems, or postprocessed for further analysis through a programming language, using one of the multiple libraries available for this end. The source code of the package developed is freely available online under the GNU GPL license at https://bitbucket.org/pysdi/pysdi.

Downloaded from http://iwaponline.com/jh/article-pdf/22/1/170/642272/jh0220170.pdf
by guest

The results of this procedure are used to derive maps and time series of drought intensity and magnitude, as well as time series of the fraction of the area affected by the different categories of the drought. These products are generated for regions defined by three different aspects: political division, water administration, and hydrography. Aimed at representing the spatial distribution of the values in each region, time series include the minimum and maximum value, and the 25th, 50th, and 75th percentiles of the data within the region.

RESULTS AND VALIDATION

Validating drought monitoring products is not an easy, nor straightforward task, given that directly measuring evidence of the severity of a drought event is virtually impossible. Alternatively, a common approach to assess the ability of an analysis to detect droughts is to qualitatively compare the timing and intensity of events detected with a given index (or set of indices) with documented impacts. For example, Palmer (1965) demonstrated the skills of the PDSI comparing the results of its methodology with the effects of historic droughts in Kansas and Iowa, in the USA. Also, Sepulcre-Canto *et al.* (2012) evaluated the skill of the CDI comparing its results with the timing of historic droughts and the variability of annual cereal yields in Europe.

In this work, two applications of the framework were implemented to validate its results. First, its drought monitoring products were compared against documented impacts and the conditions reported by the MSM during the 2015–2017 drought in East-Southwest Mexico. Second, the framework was applied to detect annual anomalies of maize yield in Mexico from 1980 to 2018. This latter analysis includes the selection of SDIs based on the strength of their correlation with the anomalies of crop yield and a quantitative validation of their drought monitoring performance using categorical indices.

Event monitoring: the 2015–2017 East-Southwest drought

From May 2015 to August 2017, a drought in the East (E) and Southwest (SW) regions of Mexico provoked costly impacts mainly in the agricultural sector, with Guerrero and Oaxaca (both in SW) being the most affected states. In the former case, impacts included the failure of 86,400 hectares of maize crops. In Oaxaca, the impacts included more than 80,200 hectares of crops, mainly of maize and sorghum, and 18,300 heads of cattle. During this long-lasting event, the storage volume of the Benito Juarez dam in Oaxaca – used for irrigation – dropped to 14% of its total capacity. Given the severity of the damages, the Federal Government issued Disaster Declarations for both states, which allowed the allocation of funds to implement response measures for the agricultural sector and urban water supply. At the end of the drought, Guerrero and Oaxaca, along with the rest of the states in the region (Hidalgo, Puebla, Tlaxcala and Veracruz in E; and Chiapas in SW) summed together 320,500 hectares of failed crop and the loss of 49,400 heads of cattle (SADER 2018a, 2018b).

Monthly maps of the SDIs were generated to compare the features of the drought events for each phase of the hydrological cycle along with the complete signal of the drought across the hydrological system. For this reason, the SDIs used include the SPI, SRI, SSI, and $MSDI_{PRS}$, while the other combinations of variables for the MSDI were omitted. To focus on capturing the monthly variation of the analyzed indicators, all the SDIs were computed for a temporal scale of 1 month. The results of the MSM, derived from the NADM maps (https://www.drought.gov/nadm/content/north-american-drought-monitor), are included along with the products of the framework introduced to visually compare the results of both systems.

In the E and SW regions, the rainy season normally starts in May; however, in June 2015, the amount of precipitation observed over a great area was significantly lower than expected. This meteorological drought was detected by the SPI (first row in Figure 4), which identified the highest intensities in the states of Chiapas and Oaxaca ($SPI_{min} = -2.16$ and -2.13, respectively; *exceptional droughts*; D4). A deficit of runoff was detected by the SRI (second row), starting simultaneously with the meteorological drought, covering a smaller area and with slightly lower, although still high, intensities ($SRI_{min} = -1.73$; *extreme drought*; D3). In July, the meteorological drought expanded to other regions, covering more than 44% of the country; however, its intensity in the studied area was lightly reduced.

Downloaded from http://iwaponline.com/jh/article-pdf/22/1/170/642272/jh0220170.pdf
by guest

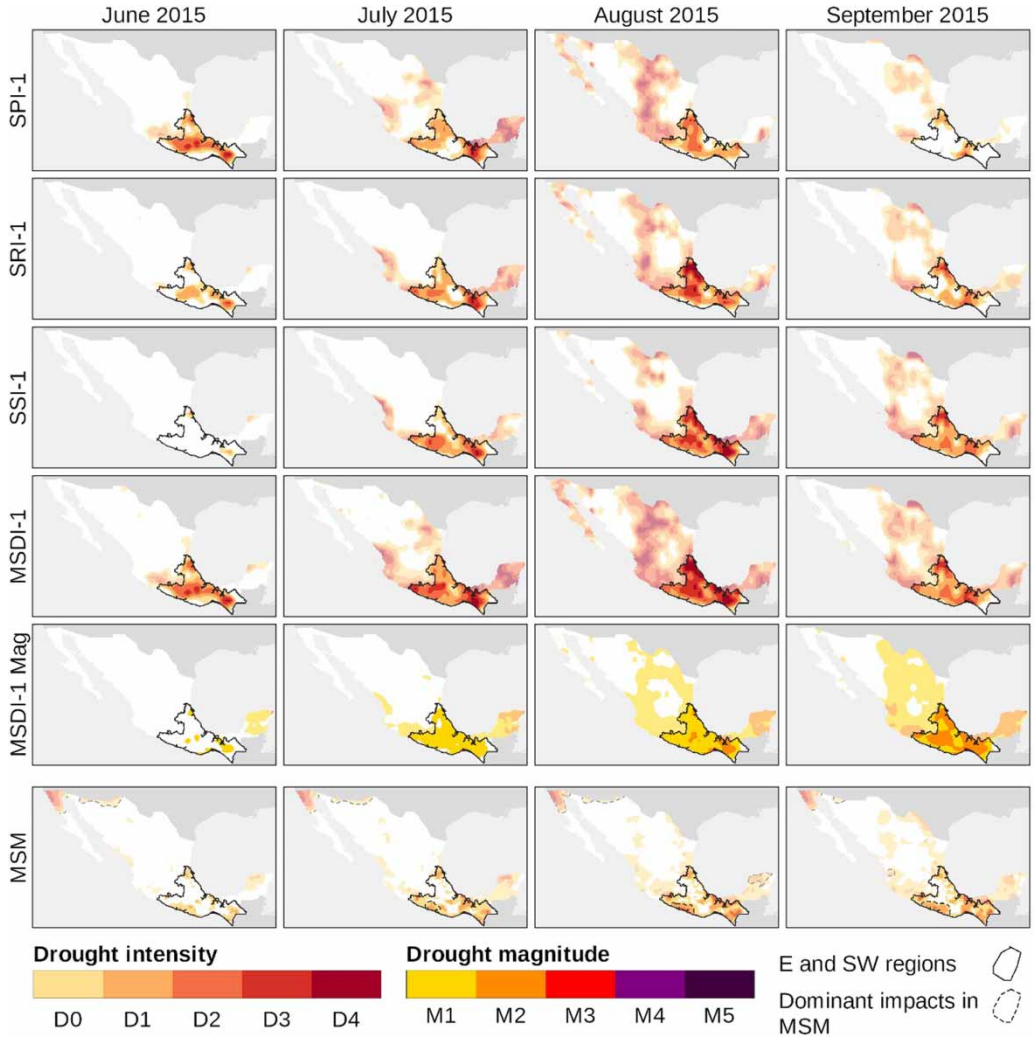

Figure 4 | Comparison of the drought maps of the framework introduced against the MSM during the onset of the Southwest 2015–2017 drought. MSM maps were composed with data from https://www1.ncdc.noaa.gov/pub/data/nidis/shapefiles/.

The runoff deficit expanded as well as the meteorological drought but, again, in a smaller area and with an attenuated intensity, comparatively. Moreover, in this month, the onset of an agricultural drought was detected with the SSI (third row) in the regions of interest, as well as in the neighboring regions, Chiapas being the state with the highest intensities, reaching values of $SSI_{min} = -2.17$ (*exceptional drought*; D4). From that moment on, runoff and soil moisture droughts closely followed the precipitation drought with a temporal lag of 1 month. The $MSDI_{PRS}$ (fourth row) shows the joint effects of the three previous variables, with deficits significantly more intense starting in July 2015, when the marginal deficits of precipitation, runoff and soil moisture are concurrently in extreme or exceptional categories.

Drought magnitude maps (fifth row in Figures 4 and 5) were derived with the drought intensity according to the $MSDI_{PRS}$ in order to capture the overall drought conditions. By means of this indicator, it is possible to detect that, although in September 2015, a great part of the country was under water deficit conditions, the drought in the E and SW regions lasted longer and had accumulated a larger deficit than the rest of the country. Moreover, it allows to identify areas where drought persisted until August 2017, even with SDIs reporting near-to-normal conditions. Here, accumulated deficit values were divided by an intensity

Downloaded from http://iwaponline.com/jh/article-pdf/22/1/170/642272/jh0220170.pdf
by guest

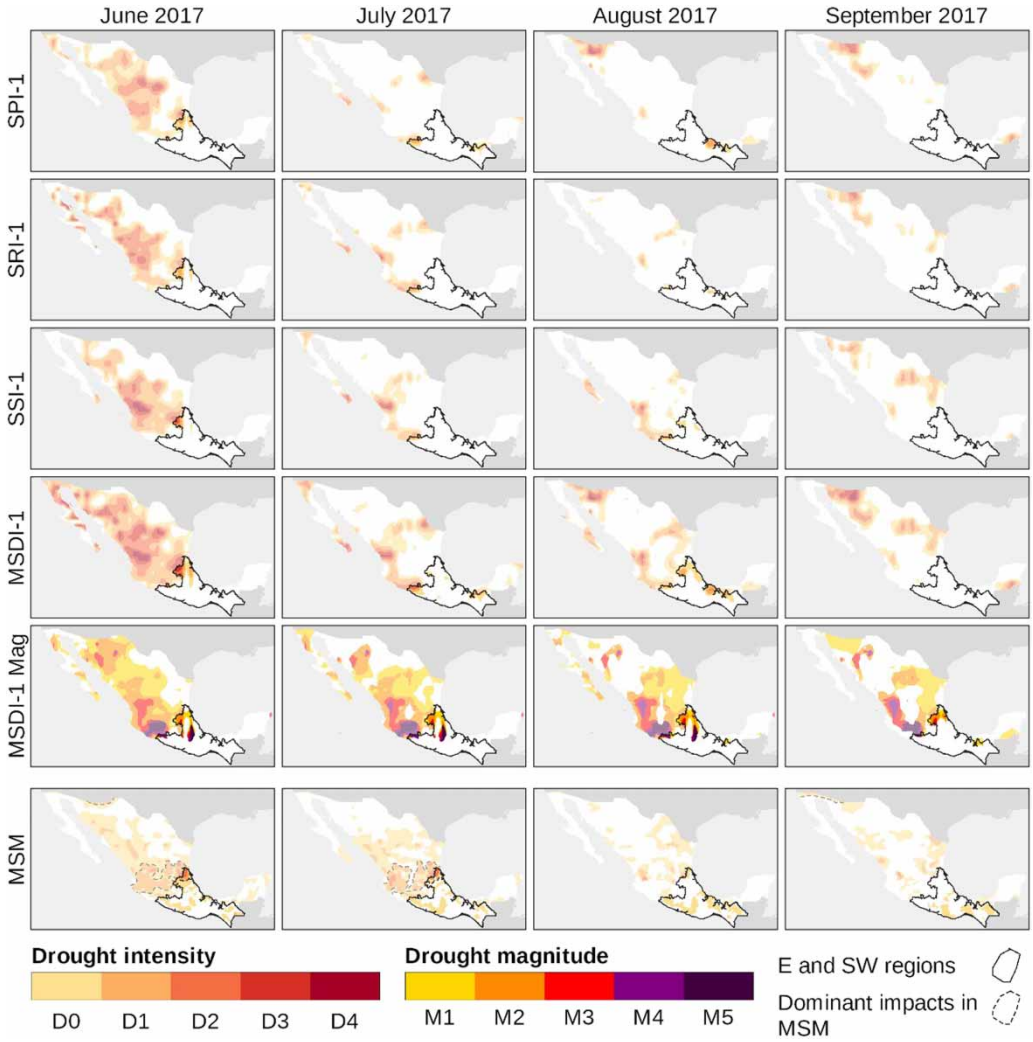

Figure 5 | Comparison of the drought maps of the framework introduced against the MSM during the termination of the Southwest 2015–2017 drought. MSM maps were composed with data from https://www1.ncdc.noaa.gov/pub/data/nidis/shapefiles/.

threshold of −1.3 to express the magnitude results in terms of the drought category 'severe' (see Table 1); however, this value might be modified to fit results to observed impacts.

The last row of Figures 4 and 5 shows MSM drought maps to contrast the results of both systems. However, the differences in the temporal scale of the inputs of each drought monitor make the comparison somewhat subjective. Drought intensities derived with the presented framework seem to systematically indicate more severe drought conditions given its temporal scale of 1 month, chosen here to track the variation of the monitored variables in the present without the influence of anomalies that occurred in the past, which may not be related to current water deficits (or excesses). Meanwhile, inputs of the MSM include the percent of the normal precipitation for temporal aggregation windows from 30 to 365 days into a single product.

The spatial and temporal distribution of the drought conditions were similarly represented by the two approaches mostly between the drought magnitude indicator and the MSM results. Nevertheless, it is worth highlighting three significant differences in the analyzed case. The first of these is outside the E and SW regions in the Northwest (NW) of Mexico. In the westernmost part of the boundary with the USA, the MSM reported severe drought conditions (Figure 4), while none of the SDIs of

Downloaded from http://iwaponline.com/jh/article-pdf/22/1/170/642272/jh0220170.pdf
by guest

the system introduced here detected deficits in that area. This difference is also assumed to be due to the differences in the temporal scale of both systems, given that when increasing the temporal scale of the analysis to 12 months, the $MSDI_{PRS}$-12 (not shown here) does detect a drought in the mentioned location. A second important difference identified in the analyzed case is in the Puebla state, near to the Gulf of Mexico, where the framework introduced here detected a severe drought that reached, in its most affected point, a magnitude of $M = 20.9$ (M5, the highest category of its classification). Meanwhile, the MSM did not report the occurrence of a drought, although reported losses in this state included more than 60,000 hectares of maize and 10,800 heads of cattle (SADER 2018b).

Figure 6 shows the time series of the SDIs, agricultural losses and storage levels in the Benito Juarez dam observed in the Oaxaca state during the period 2015–2017. Aiming to represent the distribution of the drought indices values within the state, the figure shows time series of their median values (the 50th percentile) and their interquartile range. This figure shows how the impacts on rainfed agriculture were concentrated in August–November 2015 due to the meteorological drought of June–September detected by the SPI, which coincided with the growing stage of warm season crops. Losses in irrigated agriculture were observed in October 2015, during the meteorological drought of June–September, and in April 2017, when the Benito Juarez dam storage was at its lowest level, coinciding with

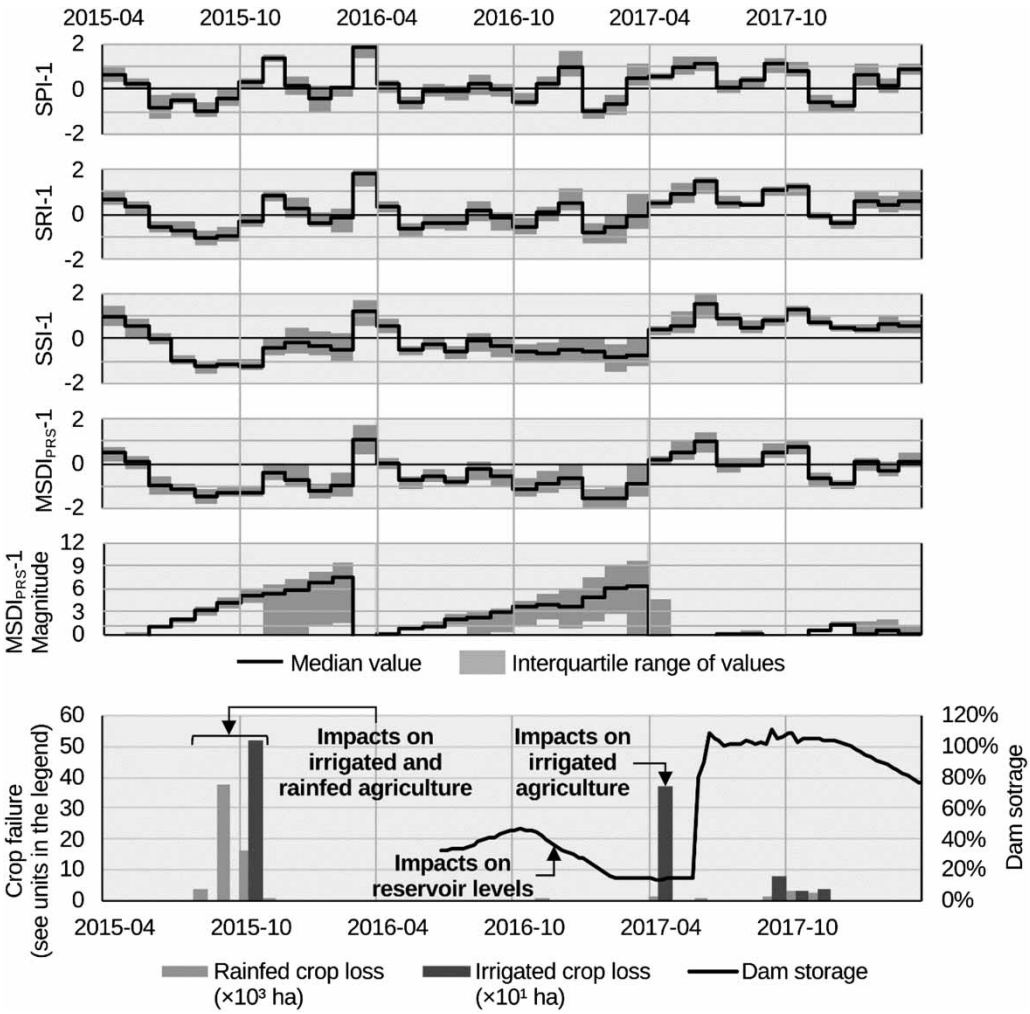

Figure 6 | SDIs with a temporal scale of 1 month and impacts reported during the 2015–2017 East-Southwest drought. Impacts data from SADER (2018a) and CONAGUA (2018).

Downloaded from http://iwaponline.com/jh/article-pdf/22/1/170/642272/jh0220170.pdf
by guest

the agricultural drought from May 2016 to March 2017 detected by the SSI.

The hydrological impacts observed in the drop of Benito Juarez dam storage were gradually aggravated from October 2016 to its critical value of 14% in February 2017. Due to lack of data before July 2016, it is difficult to distinguish how the storage correlates with the drought indices; however, a similarity with the results of the drought magnitude, given the cumulative nature of both variables, can be observed.

Evaluating annual agricultural impacts

The monitoring capabilities of the framework to detect impacts on agriculture was tested on the warm season rainfed maize annual yield in Mexico in the period 1980–2018 using data from the Agri-food and Fisheries Information Service (SIAP; http://infosiap.siap.gob.mx/gobmx/datosAbiertos_a.php) of the Ministry of Agriculture and Rural Development in Mexico (SADER). To this end, the combination of SDI, temporal scale and month of computation that better reflects the variation in the annual crop yield in each state was first determined. This included the six drought indices described in the subsection 'Drought definition', 12 different temporal scales (1, 2, …, 12 months) and the 12 months of the agricultural year of analysis. In this study, the correlation between the agricultural production of a given year and the drought conditions of previous years was not explicitly explored; however, there are cases in which the combination of temporal scale and month of computation implies including the conditions of the last months of the preceding year.

The crop yield was defined as the quantity of product harvested per unit of the planted area (in tons per hectare). Anomalies of crop yield were calculated using as a reference a locally weighted regression model, coupled with a multiplicative decomposition model (Lu Carbone & Gao 2017). The correlation between the anomalies of crop yield and SDIs was quantified with the Spearman's rank correlation coefficient (r_S), computed as follows (Zwillinger & Kokoska 2000):

$$r_S = 1 - \frac{6\sum_{i=1}^{n}(u_i - v_i)^2}{n(n^2-1)} \tag{3}$$

where u_i and v_i are the ranks of the ith value of the variables x and y, respectively; and n is the size of the sample. In order to estimate the confidence intervals of the correlations, a bivariate bootstrap approach was used. The correlation assigned to each drought index is the mean of the r_S computed for 1,000 bootstrapped samples, and the approximate lower and upper confidence limits were estimated as the $\alpha/2$ and $1-\alpha/2$ percentiles of the results, respectively (Howell 2013). The combination with the highest correlation was selected as the best indicator for drought monitoring for the rainfed maize production in each state.

To test the monitoring capabilities of the selected SDIs, each pair of values of SDI and crop yield anomaly was converted to dichotomous variables using the value of 0.0 as a threshold between negative and positive anomalies in order to apply the classifications of *hit*, *miss*, *false alarm*, and *correct negative* (Table 2).

For this evaluation, three indices were computed: the probability of detection (POD), the false alarm ratio (FAR), and the proportion correct (PC). POD computes the fraction of times when a reduction in observed crop yield was detected by the index as follows (Wilks 2006):

$$\mathrm{POD} = \frac{a}{a+c} \tag{4}$$

where a is the number of *hits* and c is the number of *misses*. The FAR quantifies the reliability of the drought indices as the fraction of times when a drought was detected by the SDI but no reduction in the crop yield was observed. The following expression is used to compute it:

$$\mathrm{FAR} = \frac{b}{a+b} \tag{5}$$

where b is the number of *false alarms*. Finally, the PC was computed to evaluate the accuracy of the SDIs. This

Table 2 | Contingency table for the detection of crop yield reduction due to droughts

	Yield reduction observed	No yield reduction observed
Drought indicated	Hit	False alarm
No drought indicated	Miss	Correct negative

Downloaded from http://iwaponline.com/jh/article-pdf/22/1/170/642272/jh0220170.pdf
by guest

metric computes the fraction of the times for which the SDI correctly represented the occurrence or not of a reduction in the crop yield as follows:

$$\mathrm{PC} = \frac{a+d}{a+b+c+d} \tag{6}$$

where d is the number of *correct negatives*. Possible values of these indices range from 0 to 1, being 1 the optimum value for PC and POD, while 0 is the optimum value for the FAR.

Table 3 shows the results of this evaluation, performed in 31 states of Mexico, with Baja California Sur being the only one excluded because it does not produce maize with rainfed agriculture. Temporal scales are denoted with a number attached to the SDI names. Results show that maize yield anomalies in 74% (23) of the states are better

Table 3 | SDI with the strongest correlation with the anomalies of the maize rainfed crop yield for each state

				r_s 95% confidence limits				
State	**SDI aggregation**	**Month of computation**	r_s	**Lower**	**Upper**	**POD**	**FAR**	**PC**
Aguascalientes	SPI-4	October	0.64	0.41	0.81	0.71	0.25	0.72
Baja California	SSI-5	May	0.69	0.44	0.86	0.65	0.08	0.72
Campeche	SRI-1	July	0.52	0.25	0.73	0.64	0.26	0.67
Chiapas	SPI-1	August	0.62	0.40	0.80	0.74	0.26	0.74
Chihuahua	SPI-5	September	0.44	0.18	0.70	0.69	0.39	0.69
Coahuila	SSI-1	August	0.40	0.12	0.65	0.70	0.26	0.72
Colima	SRI-5	April	0.55	0.30	0.75	0.67	0.20	0.69
Durango	$\mathrm{MSDI_{PS}}$-2	October	0.70	0.49	0.84	0.84	0.33	0.72
Guanajuato	SPI-6	November	0.79	0.64	0.90	0.78	0.18	0.82
Guerrero	$\mathrm{MSDI_{PS}}$-1	August	0.73	0.52	0.88	1.00	0.44	0.72
Hidalgo	SPI-1	August	0.32	0.01	0.58	0.57	0.40	0.56
Jalisco	SSI-12	November	0.67	0.46	0.83	0.67	0.33	0.69
Mexico City	$\mathrm{MSDI_{PRS}}$-6	May	0.55	0.28	0.77	0.80	0.29	0.67
Mexico State	$\mathrm{MSDI_{PS}}$-3	June	0.41	0.13	0.67	0.83	0.35	0.72
Michoacan	SPI-9	June	0.36	0.06	0.63	0.59	0.35	0.59
Morelos	$\mathrm{MSDI_{PS}}$-5	August	0.58	0.31	0.79	0.81	0.26	0.74
Nayarit	$\mathrm{MSDI_{PR}}$-1	June	0.41	0.13	0.65	0.67	0.26	0.69
Nuevo Leon	$\mathrm{MSDI_{PRS}}$-1	September	0.44	0.17	0.68	0.78	0.44	0.62
Oaxaca	SPI-2	August	0.62	0.38	0.79	0.68	0.32	0.69
Puebla	SPI-12	November	0.44	0.13	0.71	0.74	0.36	0.67
Queretaro	$\mathrm{MSDI_{PR}}$-2	September	0.50	0.21	0.71	0.76	0.30	0.69
Quintana Roo	SPI-2	February	0.53	0.25	0.76	0.67	0.26	0.69
San Luis Potosi	$\mathrm{MSDI_{PRS}}$-3	October	0.37	0.07	0.62	0.79	0.40	0.64
Sinaloa	$\mathrm{MSDI_{PS}}$-4	September	0.54	0.32	0.74	0.77	0.26	0.72
Sonora	SPI-1	August	0.47	0.15	0.71	0.50	0.35	0.55
Tabasco	SPI-3	March	0.41	0.12	0.63	0.57	0.40	0.56
Tamaulipas	SSI-2	September	0.69	0.46	0.84	0.68	0.35	0.67
Tlaxcala	SSI-1	June	0.47	0.16	0.75	0.69	0.39	0.69
Veracruz	SSI-1	June	0.47	0.17	0.71	0.71	0.43	0.64
Yucatan	SPI-2	August	0.45	0.15	0.68	0.63	0.33	0.67
Zacatecas	$\mathrm{MSDI_{PRS}}$-3	October	0.72	0.51	0.87	0.90	0.32	0.72

Downloaded from http://iwaponline.com/jh/article-pdf/22/1/170/642272/jh0220170.pdf
by guest

detected by SDIs that use precipitation as an input. This finding was unexpected; given the nature of the impacts evaluated, soil moisture was the variable expected to predominate among the other variables. However, the soil moisture is present as input in 48% (15) of the states, in the SSI and the $MSDI_{PS}$ and $MSDI_{PRS}$. In 52% (16) of the cases, the strongest correlation was found in SDIs with temporal scales of 1–2 months, which may be related to the duration of the critical period of water requirement of the corn plant in 30 days after the end of its tasseling stage, the period in which each day of water deficit may provoke a final yield reduction between 6% and 13% (Ruiz Corral *et al.* 2013).

The analysis of the drought monitoring performance of the SDIs on a national scale yielded values of FAR = 0.32, POD = 0.71, and PC = 0.68, which means that 32% of instances of impacts inferred through the SDIs were false alarms; 71% of the times that agricultural impacts were observed, they were successfully inferred through the SDIs; and 68% of inferences of the SDIs succeeded in depicting the observed conditions (impacts and no impacts observed). On the other hand, in the analysis on a state scale, 81% (25) of the states have values of FAR <0.4; 87% (27) yielded POD >0.6; and 87% (27) exhibited values of PC >0.6.

The results of this analysis are satisfactory in most of the states evaluated. However, four states are noted for their poor performance: Hidalgo, Michoacan, Sonora, and Tabasco, where applying the SDIs derived from this framework to detect drought impacts on annual maize production must be carried out considering its limitation or even avoided. The performance derived from this analysis might be constrained by the variations in the planting timing, which would hinder the possibility of using SDIs fixed in time to detect the agricultural impacts. Furthermore, the values of the SDIs used in this evaluation are computed as the median of the area in each state, while the actual rainfed agricultural surface fraction does not exceed 15% of the state surface in most cases. The analysis presented here can be refined using the drought conditions found exclusively in the agricultural surface from which the state annual production is derived. However, available data to perform such analysis in Mexico is limited to less than 16 years. Finally, the information reported in the records of the SIAP does not discriminate the impacts of droughts from other natural or biological hazards for crops, such as floods and plagues. This may affect the results of the evaluation in cases when evidence of impact is observed but no drought detected, which would be classified as a *miss* in the contingency table. Further analysis is still needed to assess the influence of these aspects in this exercise of validation.

CONCLUSIONS

In this paper, a transparent framework for drought monitoring based on global, freely available datasets is introduced. This framework characterizes drought severity based on non-parametric uni- and multivariate standardized indices, from which drought features, like duration, intensity, and magnitude, can be easily derived.

The data processing was carried out with a novel open source software package for Python that expedites the computation of the drought indices using multidimensional, multivariate datasets as input. The future development of the package (and the framework presented) includes exploring other data sources that might reduce the temporal latency of the publishing of new monitoring products, which currently is constrained to around 18–20 days due to the latency of the MERRA-2 products.

In a visual comparison of maps generated with the presented framework against drought maps of the MSM for the 2015–2017 East-Southwest drought in Mexico, the framework introduced here succeeded in reproducing the temporal and spatial distribution of the drought conditions of the MSM system, and, furthermore, it was capable of detecting regions severely affected by droughts that the MSM failed to detect. It is important to state here that, although reproducing the results of the MSM was not the target of this development, these results are encouraging, given that they demonstrate the usefulness of the framework following a transparent procedure completely based on freely available global reanalysis datasets.

In a quantitative evaluation of the framework's performance in detecting impacts on the annual maize yield through a contingency table approach, results obtained are satisfactory, with values of FAR, POD, and PC on the national scale of 0.32, 0.71, and 0.68, respectively. However,

Downloaded from http://iwaponline.com/jh/article-pdf/22/1/170/642272/jh0220170.pdf
by guest

relatively poor metrics were obtained in the states of Hidalgo, Michoacan, Sonora, and Tabasco. These results might be improved in a further analysis that should include changes in the validation procedure that allow us to fix the computation of the SDI on the growing stage of the crop. Moreover, future work includes evaluating the performance of the framework to detect drought impacts on other crops and using these results to generate a set of warning thresholds for different applications.

Among the products generated in this system, drought magnitude emerges as a key indicator of drought severity due to its ability to represent drought persistency even under low drought intensity conditions. Moreover, it has the advantage of being derived from an easy, straightforward procedure (it is the accumulated deficit during a drought).

Given its ability to detect regional and country-wide droughts on a monthly temporal scale, the introduced drought monitoring framework has become operational and complementary to the drought monitoring efforts of the Mexican government since 2016 in the Multivariate Drought Monitor of Mexico (MOSEMM), supported by CONAGUA and the Institute of Engineering of the National Autonomous University of Mexico (II-UNAM). The simplicity and transparency of this framework, together with the use of globally, freely available data as input for computing the spatial and temporal distribution of drought conditions with open source informatic tools, make it an alternative drought monitoring tool for other regions where records of hydrological variables are scarce.

REFERENCES

Adler, R. F., Huffman, G. J., Chang, A., Ferraro, R., Xie, P. P., Janowiak, J., Rudolf, B., Schneider, U., Curtis, S., Bolvin, D., Gruber, A., Susskind, J., Arkin, P. & Nelkin, E. 2003 The Version-2 Global Precipitation Climatology Project (GPCP) Monthly Precipitation Analysis (1979–present). *Journal of Hydrometeorology* **4**, 21.

Blauhut, V., Stahl, K., Stagge, J. H., Tallaksen, L. M., De Stefano, L. & Vogt, J. 2016 Estimating drought risk across Europe from reported drought impacts, drought indices, and vulnerability factors. *Hydrology and Earth System Sciences* **20** (7), 2779–2800.

CONAGUA 2018 *Almacenamiento de las Principales Presas del País (Storage in the Main Dams of the Country)*. Available from: https://www.gob.mx/conagua/documentos/almacenamiento-de-las-principales-presas-del-pais (accessed 23 August 2019).

Erhardt, T. M. & Czado, C. 2018 Standardized drought indices: a novel univariate and multivariate approach. *Journal of the Royal Statistical Society: Series C (Applied Statistics)* **67** (3), 643–664.

Farahmand, A. & AghaKouchak, A. 2015 A generalized framework for deriving nonparametric standardized drought indicators. *Advances in Water Resources* **76**, 140–145.

Gelaro, R., McCarty, W., Suárez, M. J., Todling, R., Molod, A., Takacs, L., Randles, C. A., Darmenov, A., Bosilovich, M. G., Reichle, R., Wargan, K., Coy, L., Cullather, R., Draper, C., Akella, S., Buchard, V., Conaty, A., da Silva, A. M., Gu, W., Kim, G.-K., Koster, R., Lucchesi, R., Merkova, D., Nielsen, J. E., Partyka, G., Pawson, S., Putman, W., Rienecker, M., Schubert, S. D., Sienkiewicz, M. & Zhao, B. 2017 The Modern-Era Retrospective Analysis for Research and Applications, Version 2 (MERRA-2). *Journal of Climate* **30** (14), 5419–5454.

Hao, Z. & AghaKouchak, A. 2013 Multivariate standardized drought index: a parametric multi-index model. *Advances in Water Resources* **57**, 12–18.

Hao, Z. & AghaKouchak, A. 2014 A nonparametric multivariate multi-index drought monitoring framework. *Journal of Hydrometeorology* **15** (1), 89–101.

Hao, Z. & Singh, V. P. 2015 Drought characterization from a multivariate perspective: a review. *Journal of Hydrology* **527**, 668–678.

Hao, Z., AghaKouchak, A., Nakhjiri, N. & Farahmand, A. 2014 Global integrated drought monitoring and prediction system. *Scientific Data* **1**, 140001.

Howell, D. C. 2013 *Statistical Methods for Psychology*, 8th edn. Wadsworth, Belmont, CA, USA.

Hoyer, S. & Hamman, J. J. 2017 Xarray: N-D labeled arrays and datasets in python. *Journal of Open Research Software* **5**, 10.

Kao, S. C. & Govindaraju, R. S. 2010 A copula-based joint deficit index for droughts. *Journal of Hydrology* **380** (1–2), 121–134.

Keyantash, J. A. & Dracup, J. A. 2002 The quantification of drought: an evaluation of drought indices. *Bulletin of the American Meteorological Society* **83** (8), 1167–1180.

Koster, R. D., Suarez, M. J., Ducharne, A., Stieglitz, M. & Kumar, P. 2000 A catchment-based approach to modeling land surface processes in a general circulation model: 1. model structure. *Journal of Geophysical Research: Atmospheres* **105** (D20), 24809–24822.

Lawrimore, J., Heim Jr., R. R., Svoboda, M. D., Swail, V. & Englehart, P. J. 2002 Beginning a new era of drought monitoring across North America. *Bulletin of the American Meteorological Society* **83** (8), 1191–1192.

Lobato-Sánchez, R. 2016 El monitor de sequía en México (The drought monitor in Mexico). *Tecnología y Ciencias del Agua* **7** (5), 197–211.

Lu, J., Carbone, G. J. & Gao, P. 2017 Detrending crop yield data for spatial visualization of drought impacts in the United States,

Downloaded from http://iwaponline.com/jh/article-pdf/22/1/170/642272/jh0220170.pdf
by guest

1895–2014. *Agricultural and Forest Meteorology* **237–238**, 196–208.

McKee, T. B., Doesken, N. J. & Kleist, J. 1993 The relationship of drought frequency and duration to time scales. In: *Eighth Conference on Applied Climatology*. American Meteorological Society, Anaheim, pp. 179–184.

Palmer, W. C. 1965 *Meteorological Drought*. United States Weather Bureau, Washington, DC, p. 58.

Quiring, S. M. 2009 Developing objective operational definitions for monitoring drought. *Journal of Applied Meteorology and Climatology* **48** (6), 1217–1229.

Reichle, R. H., Liu, Q., Koster, R. D., Draper, C. S., Mahanama, S. P. P. & Partyka, G. 2017a Land surface precipitation in MERRA-2. *Journal of Climate* **30** (5), 1643–1664.

Reichle, R. H., Draper, C. S., Liu, Q., Girotto, M., Mahanama, S. P. P., Koster, R. D. & De Lannoy, G. J. M. 2017b Assessment of MERRA-2 land surface hydrology estimates. *Journal of Climate* **30** (8), 2937–2960.

Rocklin, M. 2015 Dask: parallel computation with blocked algorithms and task scheduling. In: *Python in Science Conference, Presented at the Python in Science Conference*, Austin, TX, pp. 126–132.

Ruiz Corral, J. A., Medina García, G., González Acuña, I. J., Flores López, H. E., Ramírez Ojeda, G., Ortiz Trejo, C., Byerly Murphy, K. F. & Martínez Parra, R. A. 2013 *Requerimientos agroecológicos de cultivos (Agroecological Crop Requirements) (Libro técnico núm. 3)*, 2nd edn. INIFAP-CIRPAC, Tepatitlán de Morelos, Jalisco, México.

SADER 2018a *Servicio de Información Agroalimentaria y Pesquera (Agrifood and Fisheries Information Service)*. Available from: https://www.gob.mx/siap (accessed 15 January 2019).

SADER 2018b *Información histórica de sequías (Historic Information on Droughts)*. Retrieved from: https://datos.gob.mx/busca/dataset/informacion-historica-de-sequia-de-sagarpa (accessed 22 May 2019).

Sepulcre-Canto, G., Horion, S., Singleton, A., Carrão, H. & Vogt, J. V. 2012 Development of a combined drought indicator to detect agricultural drought in Europe. *Natural Hazards and Earth System Science* **12** (11), 3519–3531.

SHCP 2010 *Acuerdo por el que se emiten las Reglas Generales del Fondo de Desastres Naturales (Agreement by Which the General Rules of the Natural Disaster Fund Are Issued)*. DOF: 03/12/2010.

Shukla, S. & Wood, A. W. 2008 Use of a standardized runoff index for characterizing hydrologic drought. *Geophysical Research Letters* **35** (2), 1–7.

Smakhtin, V. U. & Schipper, E. L. F. 2008 Droughts: the impact of semantics and perceptions. *Water Policy* **10** (2), 131.

Stahl, K., Kohn, I., Blauhut, V., Urquijo, J., de Stefano, L., Acácio, V., Dias, S., Stagge, J. H., Tallaksen, L. M., Kampragou, E., van Loon, A. F., Barker, L. J., Melsen, L. A., Bifulco, C., Musolino, D., de Carli, A., Massarutto, A., Assimacopoulos, D. & van Lanen, H. A. J. 2016 Impacts of European drought events: insights from an international database of text-based reports. *Natural Hazards and Earth System Sciences* **16** (3), 801–819.

Svoboda, M. D., LeComte, D., Hayes, M. J., Heim Jr., R. R., Gleason, K., Angel, J. R., Rippey, B., Tinker, R., Palecki, M., Stooksbury, D., Miskus, D. & Stephens, S. 2002 Drought monitor. *Bulletin of the American Meteorological Society* **83** (8), 1181–1190.

Tigkas, D., Vangelis, H. & Tsakiris, G. 2014 DrinC: a software for drought analysis based on drought indices. *Earth Science Informatics* **8** (3), 697–709.

van Loon, A. F. 2013 *On the Propagation of Drought: How Climate and Catchment Characteristics Influence Hydrological Drought Development and Recovery*. PhD Thesis, Wageningen University, Wageningen, NL.

Wilhite, D. A. 2000 Drought as a natural hazard: concepts and definitions. In: *Drought: a Global Assessment*, Vol. I (D. A. Wilhite, ed.). Routledge Publishers, London, pp. 3–18.

Wilhite, D. A. & Glantz, M. H. 1985 Understanding the drought phenomenon: the role of definitions. *Water International* **10** (3), 111–120.

Wilks, D. S. 2006 *Statistical Methods in the Atmospheric Sciences*. International Geophysics Series, 2nd edn. Academic Press, Amsterdam, Boston.

WMO (ed.) 2009 *Guide to Hydrological Practices – Volume I: Hydrology – From Measurements to Hydrological Information (WMO-No. 168)*, Vol. I, 6th edn. World Meteorological Organization, Geneva, Switzerland.

WMO & GWP 2016 In: *Handbook of Drought Indicators and Indices* (M. D. Svoboda & B. A. Fuchs, eds). Integrated Drought Management Tools and Guidelines Series Integrated Drought Management Programme (IDMP), Geneva.

Wu, J., Chen, X., Gao, L., Yao, H., Chen, Y. & Liu, M. 2016 Response of hydrological drought to meteorological drought under the influence of large reservoir. *Advances in Meteorology* **2016**, 2197142.

Yevjevich, V. 1967 An objective approach to definitions and investigations of continental hydrologic droughts. *Hydrology Papers* **23** (23), 25–25.

Zwillinger, D. & Kokoska, S. 2000 *CRC Standard Probability and Statistics Tables and Formulae*. CRC Press, Boca Raton.

First received 16 January 2019; accepted in revised form 27 October 2019. Available online 11 December 2019

Downloaded from http://iwaponline.com/jh/article-pdf/22/1/170/642272/jh0220170.pdf
by guest